

Carbon–Carbon Bond Activation in Adsorbed Cyclopropane by Gas-Phase Atomic Hydrogen on the Ni(111) Surface

Adam T. Capitano, Kyung-Ah Son, and John L. Gland*

University of Michigan, Department of Chemistry, Ann Arbor, Michigan 48109-1055

Received: September 28, 1998

Gas-phase atomic hydrogen induces C–C bond activation in adsorbed cyclopropane on the Ni(111) surface, while coadsorbed hydrogen does not. Propane is the only desorbing product observed during subsequent temperature-programmed desorption experiments. Three propane formation pathways are observed. Gas-phase atomic hydrogen reacts with adsorbed cyclopropane to form intermediates at 105 K, which are hydrogenated by coadsorbed hydrogen to form propane at 116 and 210 K. The 116 K pathway is similar to previous results obtained on the Ni(100) surface where propyl was determined to be the primary intermediate. The 210 K pathway has no analogue on the Ni(100) surface and is thought to involve a more stable form of propyl on the Ni(111) surface. The reaction of subsurface hydrogen with adsorbed cyclopropane leads to propane formation at 170 K on the Ni(111) surface. The absence of methane and ethane formation indicates that no multiple C–C bond activation processes occur. In contrast, cyclopropane desorption occurs before sufficient thermal energy is available to induce C–C bond breaking with coadsorbed hydrogen.

Introduction

Understanding carbon–carbon bond activation at the molecular level is important from both technological and basic chemical perspectives. From a catalysis viewpoint, understanding the mechanisms of C–C bond activation may suggest ways to improve catalysts for processing fuels and chemicals.¹ From a basic research perspective, a molecular understanding of C–C bond activation on surfaces will provide new insight into an important class of elementary reaction processes.² Since cyclopropane is a highly strained molecule, carbon–carbon bond activation is a highly thermodynamically favorable reaction.³ The carbon–carbon bond activation mechanism in cyclopropane has been characterized using fundamental quantum chemical modeling,⁴ by studying the reactivity of organometallic clusters,⁵ and by characterizing the reactivity of a range of catalytic materials.⁶ Cyclopropane ring opening induced by hydrogen on surfaces is widely accepted as a model for catalytic carbon–carbon activation.⁷ This reaction has been used to probe the C–C bond activation site on a range of metal single-crystal and supported metal catalysts.

Unfortunately, the molecular characterization of cyclopropane ring opening using powerful vacuum-based methods has been limited since cyclopropane tends to desorb from metal surfaces before reacting with coadsorbed hydrogen.⁸ Son et al. found that gas-phase hydrogen radicals react with adsorbed cyclopropane on the Ni(100) surface even at low temperature.⁹ In this case, C–C bond activation results in the formation of an adsorbed propyl intermediate. Upon heating, the propyl was hydrogenated by coadsorbed hydrogen to form propane, which desorbs at 116 K. Thus, gas-phase atomic hydrogen induced cyclopropane ring opening provides a direct way to synthesize adsorbed propyl, which is an important intermediate for a range of surface reactions.¹⁰

In addition to C–C bond activation, the chemistry of gas-phase atomic hydrogen has been investigated for several other systems.¹¹ Despite the range of chemical reactions that has been

explored, systematic studies of the role of surface structure on the reactions of gas-phase atomic hydrogen have not been reported. This paper compares the reaction of gas-phase atomic hydrogen with cyclopropane on the Ni(111) and Ni(100) surfaces. These studies directly compare the reactivity of cyclopropane on two different surface sites.

Experimental

All experiments were performed in an ultrahigh vacuum chamber equipped with turbo, ion, and TSP pumps, which combined to give a base pressure of 5×10^{-10} Torr. The system was equipped with a quadrupole mass spectrometer (QMS) for temperature-programmed reaction spectroscopy (TPRS), Auger electron spectroscopy (AES) to verify surface cleanliness, and an atomic hydrogen source for the production of gas-phase atomic hydrogen.

A Ni(111) single metal crystal oriented within 0.5° of the low index plane was mounted on a ceramic support with two 0.5 mm tantalum wires, which allowed heating to 1050 K and liquid nitrogen cooling to 110 K. The sample was attached to an L-shaped manipulator that allows three-coordinate displacements and 360° rotation. This allowed exact positioning in front of all instruments and gas dosers. Temperature was measured with a 0.01 mm chromel–alumel (type K) thermocouple spot welded to the back of the crystal.

The crystal was cleaned by Ar^+ ion sputtering followed by annealing to 1000 K. During experimental runs, carbonaceous impurities generated by cyclopropane decomposition were the only contaminants. Comparing the amount of hydrogen produced by cyclopropane dehydrogenation to a calibration curve of a hydrogen saturated Ni(111) surface indicates that only 0.05 monolayers of cyclopropane undergoes dehydrogenation during a TPD cycle. This carbon was removed before each new TPRS experiment using Ar^+ sputtering. Auger electron spectroscopy was used to verify that the surface was clean before each experiment.

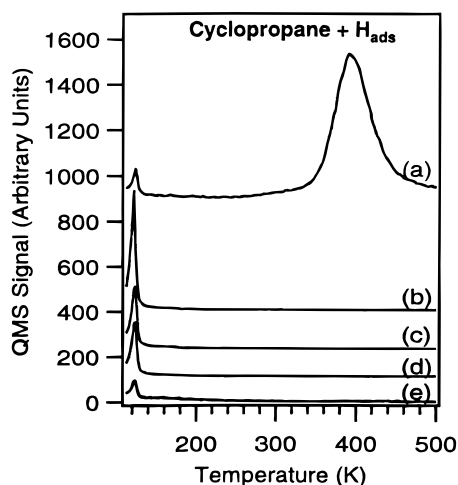


Figure 1. Coadsorption of surface hydrogen (5 langmuirs) and cyclopropane (0.36 langmuirs) results in molecular cyclopropane desorption. No propane formation is observed on the Ni(111) surface. The desorbing species are: (a) hydrogen ($m/e = 2$); (b) cyclopropane ($m/e = 42$); (c) methane ($m/e = 16$); (d) ethane ($m/e = 30$); (e) propane ($m/e = 29$).

Reactive gases were inlet through a directional dosing system controlled by a leak valve. Hydrogen (Matheson 99.9999%), deuterium (Matheson 99.5%), and cyclopropane (Matheson 99%) were used without further purification. Gas-phase atomic hydrogen was generated by passing molecular hydrogen over a 2100 K tungsten filament positioned 10 cm from the sample. We refer to the mixture of hydrogen atoms and molecules as gas-phase atomic hydrogen for simplicity. Details of this method of hydrogen atom creation are presented elsewhere.¹² All exposures are expressed in terms of langmuirs (1 langmuir = 1×10^{-6} Torr s) based on ionization gauge pressure readings and have not been corrected for large directional dosing fluxes and ion gauge sensitivity factors. All studies were performed with a saturated cyclopropane surface. For the Ni(111) surface, a 0.36 langmuirs exposure was shown to be sufficient to achieve saturation.

TPRS spectra were taken with a QMS adjusted to a low ionization energy of 30 eV to decrease the yield of hydrogen relative to organics. A Hunt scientific control system allowed the simultaneous detection of up to eight masses with independent control of mass spectrum electron multiplier sensitivities. Desorption products were identified by prominent features in their mass spectrum fragmentation patterns.¹³ For all experiments, a linear heating rate of 5 K/s was used.

Results

In the presence of coadsorbed surface hydrogen, no carbon–carbon bond activation in cyclopropane is observed on the Ni(111) surface. The TPRS results from the coadsorption of cyclopropane (0.36 langmuirs) with surface hydrogen (5 langmuirs) are shown in Figure 1. As seen in the mass 42 amu TPRS, cyclopropane is bound weakly to the Ni(111) surface and desorbs at 116 K. Using the method described by Redhead, an activation energy of 6.7 kcal/mol was estimated.¹⁴ The propane ($m/e = 29$), methane ($m/e = 15$), and ethane ($m/e = 30$) peaks all have small features at 116 K. The relative sizes of these peaks compared to the cyclopropane main peak are consistent with the fragmentation of cyclopropane in the mass spectrometer. Therefore, no single or multiple carbon–carbon bond activation is observed. Two hydrogen ($m/e = 2$) TPRS peak are observed at 116 and 400 K. The low-temperature peak

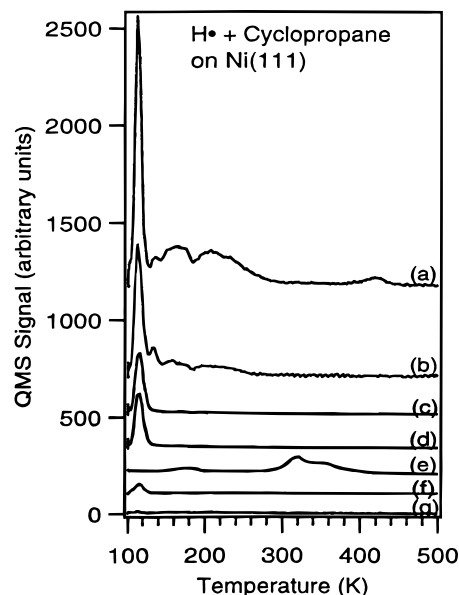


Figure 2. An initial dose of 0.36 langmuirs of cyclopropane was exposed to 210 langmuirs of gas-phase atomic hydrogen. Propane formation occurs at 116, 170, and 210 K. The desorbing species are: (a) propane ($m/e = 29$); (b) propane ($m/e = 44 \times 10$); (c) cyclopropane ($m/e = 41$); (d) cyclopropane ($m/e = 42$); (e) hydrogen ($m/e = 2 \times 0.125$); (f) methane ($m/e = 15 \times 10$); (g) ethane ($m/e = 30$).

is from cyclopropane fragmentation, while the 400 K peak results from the desorption of the 5 langmuirs of unreacted coadsorbed hydrogen.¹⁵

As can readily be seen by the substantial propane peaks in Figure 2, gas-phase atomic hydrogen induces carbon–carbon bond activation in cyclopropane adsorbed on the Ni(111) surface. This figure shows the TPRS resulting from the exposure of 0.36 langmuirs of cyclopropane to 290 langmuirs of gas-phase atomic hydrogen. Two new features at 170 and 210 K in the propane 29 and 44 amu desorption traces clearly demonstrate that propane formation occurs. In addition, propane formation at 116 K is indicated by the increase in the 29 and 44 amu TPRS peaks relative to the cyclopropane fragmentation QMS intensities. Careful examination of the 44 amu fragment at 116 K shows an intensity that is 15% greater than the expected intensity resulting from the natural abundance of ^{13}C in cyclopropane (compare Figures 1 and 2). Similarly, an increase in the propane ($m/e = 29$) peak is observed. Taken together, the increase for these two masses indicates that propane formation is occurring at 116 K. With increasing gas-phase atomic hydrogen exposure, the intensity of the 116 K feature in both the 44 and 29 amu traces increases, indicating that cyclopropane fragmentation alone is not responsible for the intensity of this peak (e.g., see Figures 4 and 5 for analysis of 29 amu). Similar observations were reported for the reaction of cyclopropane with gas-phase atomic hydrogen to form propane on the Ni(100) surface.¹⁶ On that surface, a combination of TPRS and HREELS clearly identified a propyl intermediate resulting from exposure of gas-phase atomic hydrogen to adsorbed cyclopropane. Since identical propane desorption temperatures are observed on the Ni(111) surface, by analogy, we propose a propyl intermediate.

Also in Figure 2, peaks corresponding to desorbing cyclopropane and hydrogen are observed. The cyclopropane ($m/e = 42$ amu) peak is less intense than the cyclopropane peak shown in Figure 1. As observed in Figure 1, the small desorption features at 116 K for $m/e = 2$, 15, and 30 are mass spectrometer fragments of cyclopropane. In addition to the 116 K cyclopro-

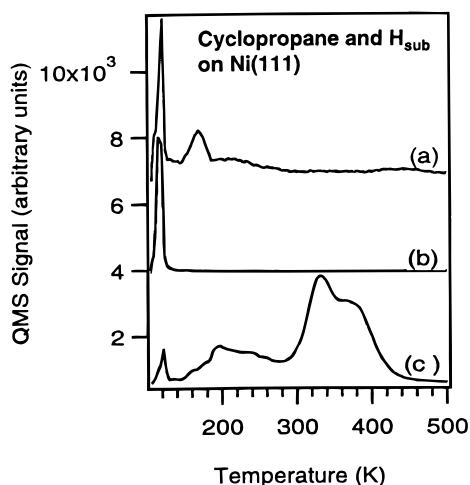


Figure 3. Subsurface hydrogen was formed by dosing 290 langmuirs of gas-phase atomic hydrogen; then, the surface was postexposed to 0.36 langmuirs of cyclopropane. Subsurface hydrogen induces propane formation at 170 K. The desorbing species are: (a) propane ($m/e = 29 \times 10$); (b) cyclopropane ($m/e = 42$); (c) hydrogen ($m/e = 2$).

pane fragment, the hydrogen ($m/e = 2$) TPRS trace has features at 170, 280, and 400 K. The 170 K peak results from the exposure of hydrogen radicals to the Ni surface and has been identified as subsurface hydrogen.¹⁷ The higher temperature peaks are the well-known β_1 and β_2 surface hydrogen desorption states that are formed from high hydrogen exposures.¹⁵ When *gas-phase cyclopropane* is exposed to gas-phase atomic hydrogen, propane, propene, and cyclopropyl radicals are formed.¹⁸ Consequently, the possibility of propene desorption was carefully investigated. Comparison of the TPRS traces at 41 and 42 amu shows that propene is not detected.

When cyclopropane is adsorbed on the Ni(111) surface predosed with gas-phase atomic hydrogen, propane formation at 170 K is observed. Figure 3 shows the results of predosing 290 langmuirs of gas-phase atomic hydrogen to the Ni(111) surface followed by exposure of 0.36 langmuirs of cyclopropane. A single propane formation peak at 170 K is observed in the propane 29 and 44 amu TPRS traces. This peak is correlated with the subsurface hydrogen state at 170 K and is discussed in detail elsewhere.¹⁹ From examination of the methane and ethane peaks, no multiple C–C bond cleavage is observed. As expected, a single cyclopropane ($m/e = 42$) peak at 116 K is observed.

With increasing gas-phase atomic hydrogen exposure, the amount of propane formation increases while less cyclopropane desorbs from the surface. The TPRS resulting from increasing hydrogen atom exposure to a cyclopropane-saturated surface is shown in Figure 4. The left side of Figure 4 shows propane 29 amu TPRS peaks for gas-phase atomic hydrogen exposures ranging from 0 to 300 langmuirs. With increasing hydrogen atom exposure, all three propane formation peaks increase in intensity. The right side of Figure 4 shows the corresponding cyclopropane ($m/e = 42$) desorption peaks. With increasing gas-phase atomic hydrogen exposure, these peaks decrease in intensity. Following the highest exposure of gas-phase atomic hydrogen, 80% of the original cyclopropane has been removed from the surface.

As clearly shown in Figure 5, the extent of propane formation correlates inversely with the amount of cyclopropane desorbing after reaction. Figure 5 compares the yields of the desorbing cyclopropane and the 116 K propane formation pathways. The intensity of the 29 amu peak was corrected for the cyclopropane contribution to obtain a more accurate propane yield. With

increasing gas-phase atomic hydrogen exposure, the amount of desorbing cyclopropane decays exponentially. Concurrently, propane yield increases exponentially indicating a first-order reaction. The same exponential was used to fit both the cyclopropane and propane data, confirming that the 116 K propane formation peak is the dominant one. In combination with Figure 2, these results clearly confirm propane formation at 116 K.

In Figure 6, the corrected propane yield induced by increasing hydrogen atom exposure shows that the 116 K state is the dominant propane formation pathway. Approximately 70% of the total propane yield comes from this state. Examination of the yields for the three propane pathways further suggests that different processes are responsible for propane formation. The 116 K state increases exponentially with increasing gas-phase atomic hydrogen exposure. In contrast, the 210 K pathway increases approximately linearly, suggesting a different mechanism for propane formation. The propane formation curve from reaction with subsurface hydrogen has an induction period. This initial induction period is consistent with both the small concentration of subsurface hydrogen formed with lower gas-phase atomic hydrogen exposure and competition with the dominant 116 K propane reaction pathway.

Comparison of these results from the Ni(111) surface with previous results from the Ni(100) surface indicates an additional propane formation pathway is observed at 210 K. The propane ($m/e = 29$) TPRS traces from similar exposures of gas-phase atomic hydrogen to adsorbed cyclopropane on the Ni(111) and Ni(100) surfaces are shown in Figure 7. On the Ni(100) surface, only two desorption features at 116 and 170 K are observed (peaks a and b). The TPRS trace corresponding to the Ni(111) surface has an additional feature at 210 K (peak c) not observed on the Ni(100) surface.

Discussion

Coadsorbed hydrogen does not induce ring opening in coadsorbed cyclopropane on the Ni(111) surface. This result contrasts with results under catalytic conditions, where the reaction of cyclopropane with hydrogen is facile.¹⁰ Although ring opening is thermodynamically favorable, the activation energies necessary to achieve reaction are higher than cyclopropane desorption energies on the Ni(111) surface. For example, the activation energy for reaction on Ni(111) was determined by Goodman et al. to be 14 kcal/mol under catalytic conditions, while the energy for desorption determined in this paper is 6.7 kcal/mol.²⁰ Therefore, in the absence of gas-phase cyclopropane, desorption occurs before the activation barrier for ring opening can be overcome. However, under catalytic conditions, gas-phase cyclopropane continually populates the surface so that sufficient cyclopropane is present to react, even though each cyclopropane has a small residence time.²¹

In contrast to coadsorbed hydrogen, gas-phase atomic hydrogen induces propane formation in cyclopropane under UHV conditions on the Ni(111) surface. TPRS results show that propane was the only reaction product from the reaction of gas-phase atomic hydrogen and cyclopropane. As seen in Figure 2, propane formation occurs via three reaction pathways. To understand the mechanisms for these reactions, a comparison to the reaction of gas-phase atomic hydrogen with cyclopropane on the Ni(100) surface can be used.⁹

On Ni(100), cyclopropane reacts with gas-phase atomic hydrogen to form propane through two mechanisms.^{9,16} The first is direct reaction of the incoming hydrogen radical with cyclopropane through an Eley–Rideal mechanism to form a

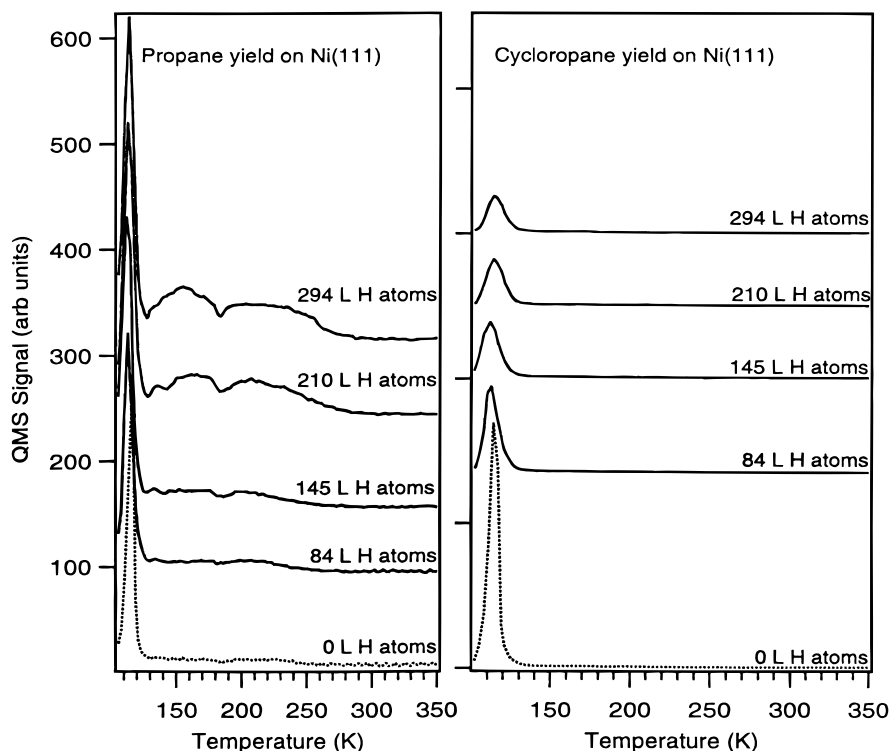


Figure 4. Effects of increasing gas-phase atomic hydrogen exposure on propane formation and cyclopropane loss. With increasing H^\bullet exposure, all three propane peaks increase and the cyclopropane peak decreases. Following a 294 langmuir exposure of gas-phase atomic hydrogen, 80% of the original cyclopropane has been removed.

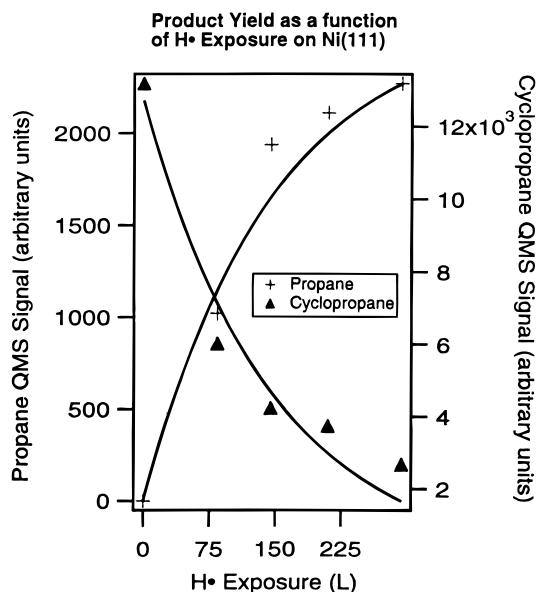


Figure 5. With increasing gas-phase atomic hydrogen exposure, the amount of desorbing cyclopropane decreases while the yield of the 116 K propane formation peak increases. The exponential decrease in cyclopropane desorption is inversely related to the exponential increase in propane yield as expected for the dominant product in a first-order reaction.

propyl intermediate. This alkyl intermediate then undergoes hydrogenation at 120 K to form propane, which desorbs. The second mechanism for propane formation involves the reaction of subsurface hydrogen with adsorbed cyclopropane at 170 K to form a propyl species. This propyl is quickly hydrogenated to form propane, which desorbs.

The first two propane formation pathways on Ni(111) (Figures 2–5) parallel the chemistry observed on the Ni(100) surface. Predosing gas-phase atomic hydrogen to form subsurface

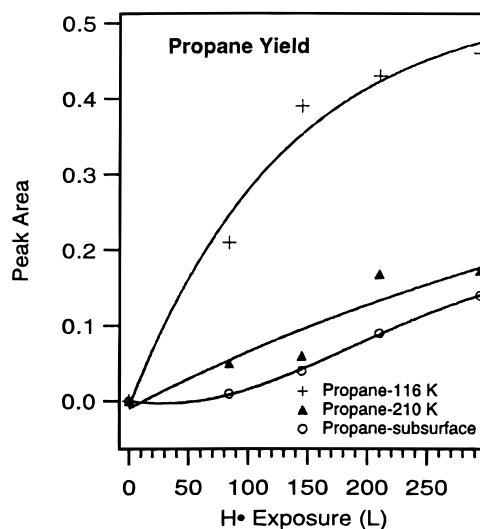


Figure 6. Yield of the three propane formation pathways increases as a function of increasing gas-phase atomic hydrogen exposure. The majority of the desorbing propane is formed by the 116 K channel. With increasing gas-phase atomic hydrogen exposure, the amount of propane formed in the 116 K pathway increases exponentially. The 170 and 210 K propane formation pathways increase less rapidly than the 116 K pathway as expected for independent mechanisms.

hydrogen leads to propane formation at 170 K in postdosed cyclopropane. Exposure of gas-phase atomic hydrogen to cyclopropane also leads to a low-temperature propane formation state at 116 K. As seen in Figures 5 and 6, the propane yield of the 116 K peak scales with increasing gas-phase atomic hydrogen exposure. Similarly, on the Ni(100) surface, larger hydrogen atom exposures lead to increased propane formation. Since both the desorption temperature and reactivity trends are similar to the Ni(100) results, we propose a similar mechanism involving the formation of a propyl intermediate on this surfaces.

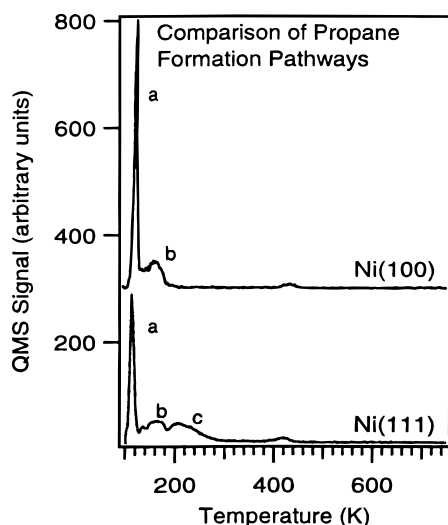


Figure 7. Comparison of the reaction of gas-phase atomic hydrogen with adsorbed cyclopropane on the Ni(111) and Ni(100) surfaces. On the Ni(100) surface, two propane formation peaks are observed: the first (a) results from direct reaction of gas-phase atomic hydrogen to form a propyl intermediate, the second (b) results from reaction with subsurface hydrogen. On the Ni(111) surface, in addition to pathways a and b, a new propane formation pathway (c) is observed at higher temperatures.

However, on the Ni(111) surface, a third propane formation pathway at 210 K is observed in addition to the two peaks observed on the Ni(100) surface. Since this state is not observed when the Ni(111) surface is predosed with gas-phase atomic hydrogen to form subsurface hydrogen (Figure 4), it must result from the direct interaction of gas-phase hydrogen radicals. The propane yield for the three pathways (Figure 7) is quite different over the entire range of gas-phase atomic hydrogen exposures. The increase in propane yield with increasing gas-phase atomic hydrogen exposure is also quite different for the three pathways. On the Pt(111) surface, three propane formation pathways were also observed for the reaction of gas-phase atomic hydrogen with adsorbed cyclopropane.²² The third, higher temperature propane formation state was attributed to hydrogenation of a strongly bound propyl intermediate. On the basis of this previous assignment, we attribute the 210 K propane formation state to a propyl group bound to a different surface site. Although the hydrogenation of propyl adsorbed on Ni(111) has not yet been studied, hydrogenation of several analogous adsorbed species support this proposal. Ab initio calculations for methyl adsorbed on Ni(111) predict that methyl is more stable in the three-fold hollow compared to the on top site by 5 kcal/mol.²³ This is consistent with HREELS studies that have assigned the adsorbed methyl to the three-fold site on Ni(111).²⁴ Recent studies for the reaction of methyl with surface hydrogen have shown that methane is produced at 250 K.²⁵ Studies of the C₁–C₃ alkyl groups on the Ni(100) surface have shown that the hydrogenation temperature to form the corresponding alkane decreases with increasing chain length.²⁶ Since the reactivity trends for the Ni(111) surface are expected to be similar, we propose that the 210 K propane formation pathway is caused by hydrogen addition to propyl adsorbed in the more stable three-fold hollow site. Similarly, we assign the 116 K state to the hydrogenation of a propyl intermediate in the on top site.

Conclusions

Surface morphology plays a significant role in the reactions of gas-phase atomic hydrogen with adsorbed cyclopropane. The

dominant 116 K pathway is similar to previous results obtained on the Ni(100) surface where propyl was determined to be the primary intermediate. The reaction of subsurface hydrogen with adsorbed cyclopropane is also similar to results on the Ni(100) surface leading to propane formation at 170 K. By altering the crystallographic orientation of the nickel surface, a new propane formation pathway is observed. The 210 K pathway has no analogue on the Ni(100) surface and is thought to involve a more stable form of propyl adsorbed on the 3-fold hollow site of the Ni(111) surface.

References and Notes

- (1) Jachnimowski, T. A.; Weinberg, W. H. *Surf. Sci.* **1997**, 370, 71.
- (2) Hall, R. B.; Kaldor, A. *J. Chem. Phys.* **1979**, 70, 4027.
- (3) Steel, C.; Zand, R.; Hurwitz, P.; Cohen, S. G. *J. Am. Chem. Soc.* **1964**, 86, 679.
- (4) Cyclopropane modeled: (a) Siegbahn, P. E. M.; Blomberg, M. R. *A. J. Am. Chem. Soc.* **1992**, 114, 10548. (b) Dewar, M. J. S. *J. Am. Chem. Soc.* **1984**, 106, 669. (c) Wong, H. N. C.; Hon, M. Y.; Tse, C. W.; Yip, Y. C.; Tanko, J.; Hudlicky, T. *Chem. Rev.* **1989**, 89, 165.
- (5) Cyclopropane with metal cluster. (a) Ni(0): Noyori, T.; Odagi, T.; Takaya, J. *J. Am. Chem. Soc.* **1970**, 92, 5780. (b) Pt(0): Rajaram, J.; Ibers, J. A. *J. Am. Chem. Soc.* **1978**, 100, 829. (c) Pt(II): Al-Essa, R. J.; Puddephatt, R. J.; Thompson, P. J.; Tipper, C. F. H. *J. Am. Chem. Soc.* **1980**, 102, 7546.
- (6) (a) Huang, C. P.; Richardson, J. T. *J. Catal.* **1978**, 52, 332. (b) Verma, A.; Ruthven, D. V. *M. J. Catal.* **1977**, 46, 160. (c) Della Betta, R. A.; Cusumano, J. A.; Sinfelt, J. H. *J. Catal.* **1970**, 19, 343. (d) Kahn, D. R.; Petersen, E. E.; Somorjai, G. A. *J. Catal.* **1974**, 34, 294. (e) Engstrom, J. R.; Goodman, D. W.; Weinberg, W. H. *J. Phys. Chem.* **1990**, 94, 396.
- (7) Wittrig, T. S.; Szuromi, P. D.; Weinberg, W. H. *J. Chem. Phys.* **1982**, 76, 716.
- (8) Wittrig, T. S.; Szuromi, P. D.; Weinberg, W. H. *Surf. Sci.* **1982**, 116, 414.
- (9) Son, K. A.; Gland, J. L. *J. Am. Chem. Soc.* **1996**, 118, 10505.
- (10) Sridhar, T. S.; Ruthven, D. M. *J. Catal.* **1972**, 24, 153.
- (11) Cyclohexene on Cu(100): (a) Teplyakov, A. V.; Bent, B. E. *J. Chem. Soc., Faraday Trans.* **1995**, 91, 3645. (b) Cyclohexene on Ni(100): Son, K. A.; Mavrikakis, M.; Gland, J. L. *J. Phys. Chem.* **1995**, 99, 6270. (c) Ethylene on Ni(100): Daley, S. P.; Utz, A. L.; Trautman, T. R.; Ceyer, S. T. *J. Am. Chem. Soc.* **1993**, 116, 6001. (d) Ethylene on Cu(100): Yang, M. X.; Bent, B. E. *J. Phys. Chem.* **1996**, 100, 822. (e) CH₃I on Cu(100): Park, Y. S.; Kim, J. Y.; Lee, J. *Surf. Sci.* **1996**, 363, 62.
- (12) Energetic Hydrogen Atom induced carbon–carbon bond activation in small cycloalkanes (C_nH_{2n}, n = 3, 4, 5, & 6) on the Ni(100) surface. Son, K. A. Doctoral Thesis, University of Michigan, 1996.
- (13) National Institute of Standards and Technology world wide web site, <http://webbook.nist.gov/chemistry/>, and comparison to fragmentation patterns obtained in our mass spectrometer.
- (14) Redhead, P. A. *Vacuum* **1962**, 12, 203.
- (15) Christman, K.; Schober, O.; Ertl, G.; Neumann, M. *J. Chem. Phys.* **1974**, 60, 4528.
- (16) Son, K. A.; Gland, J. L. *J. Am. Chem. Soc.* **1995**, 117, 5415.
- (17) Johnson, A. D.; Daley, S. P.; Utz, A. L.; Ceyer, S. T. *Science* **1992**, 257, 223.
- (18) (a) Marshall, R. M.; Purnell, H.; Sheppard, A. *J. Chem. Soc., Faraday Trans. 2* **1986**, 82, 929. (b) Marshall, R. M.; Purnell, H.; Satchell, P. W. *J. Chem. Soc., Faraday Trans. 1* **1984**, 80, 2395.
- (19) Capitano, A. T.; Gland, J. L. *Langmuir* **1998**, 14, 1345.
- (20) Goodman, D. W. *J. Vac. Sci. Technol. A* **1984**, 2, 873.
- (21) Somorjai, G. A. *Introduction to Surface Chemistry and Catalysis*; John Wiley and Sons: New York, 1994; p 302.
- (22) Capitano, A. T.; Gland, J. L. *J. Phys. Chem. B* **1998**, 102, 2562.
- (23) (a) Yang, H. Y.; Whitten, J. L. *J. Am. Chem. Soc.* **1991**, 113, 6442. (b) Yang, H. Y.; Whitten, J. L. *Surf. Sci.* **1991**, 225, 193.
- (24) Lee, M. B.; Yang, Q. Y.; Ceyer, S. T. *J. Chem. Phys.* **1987**, 87, 2742.
- (25) Tjandra, S.; Zaera, F. *J. Catal.* **1994**, 147, 598.
- (26) (a) Methyl on Ni(100): Tjandra, S.; Zaera, F. *J. Catal.* **1993**, 144, 361. (b) Ethyl on Ni(100): Tjandra, S.; Zaera, F. *Surf. Sci.* **1993**, 289, 225. (c) Propyl and higher alkyls on Ni(100): Tjandra, S.; Zaera, F. *J. Phys. Chem.* **1994**, 98, 3044.